MedChemComm

CONCISE ARTICLE

View Article Online
View Journal

Cite this: DOI: 10.1039/c5md00357a

Acetophenone derivatives: novel and potent small molecule inhibitors of monoamine oxidase B†

Zhi-Min Wang, Xue-Mei Li, Wei Xu, Fan Li, Jin Wang, Ling-Yi Kong* and Xiao-Bing Wang*

Received 20th August 2015,
Accepted 5th October 2015

DOI: 10.1039/c5md00357a

www.rsc.org/medchemcomm

Two series of acetophenone derivatives have been designed, synthesized and evaluated for human monoamine oxidase A and B inhibitory activity *in vitro*. Most of the tested compounds acted preferentially on MAO-B with IC_{50} values in the nanomolar range and weak or no inhibition of MAO-A. In particular, compounds **1j** (IC_{50} = 12.9 nM) and **2e** (IC_{50} = 11.7 nM) were the most potent MAO-B inhibitors being 2.76- and 2.99-fold more active than selegiline. In addition, the structure–activity relationships for MAO-B inhibition indicated that substituents at C3 and C4 of the acetophenone moiety, particularly with the halogen substituted benzyloxy, were more favorable for MAO-B inhibition. Molecular docking and kinetic studies have been carried out to explain the binding modes of MAO-B with the acetophenone derivatives. Furthermore, the representative compounds **1j** and **2e** showed low neurotoxicity in SH-SY5Y cells. It may be concluded that the acetophenone derivatives could be used to develop promising lead compounds for treating neurodegenerative diseases.

Introduction

Monoamine oxidase (MAO, EC 1.4.3.4) is a flavoenzyme that plays an essential role in the regulation and metabolism of amine neurotransmitters in the peripheral tissues and central nervous system (CNS).[1,2] Two isoforms of MAOs have been identified in mammals and named MAO-A and MAO-B, which were recognized on account of differences in immunological properties, inhibitor specificity, amino acid sequences, substrate preference and tissue distribution.[3–5] MAO-A displays higher affinity for the substrates norepinephrine and serotonin (5-HT) than MAO-B and is inhibited by low concentrations of clorgyline and preferentially metabolizes epinephrine, 5-hydroxytryptamine (5-HT) and norepinephrine (NE), whereas MAO-B exhibits higher affinity toward benzylamine and phenylethylamine (PEA) and is potently inhibited by selegiline and rasagiline. Both enzymes can metabolize tryptamine, dopamine (DA) and tyramine.[6–9]

Recent studies on crystal structures of the two MAO isoforms provide information about the pharmacophoric requirements and the selective interactions, which are useful to design potent and selective inhibitors.[10] MAO-A has a single hydrophobic cavity. On the contrary, the active site of MAO-B consists of two distinct cavities: one is the so-called "entrance cavity", which is located towards the outside of the protein, and another larger cavity called "substrate cavity" is connected to the flavin adenine dinucleotide cofactor (FAD). There are narrow pockets in these cavities of both isoenzymes, and the Tyr 326 and Ile 199 residues in MAO-B act as a bottleneck and thus form a gate, which separates the region as two cavities.[11,12]

Since the main role of the MAOs in the CNS is to terminate the actions of neurotransmitter amines, they are considered attractive drug targets for the treatment of psychiatric and neurological disorders. Selective inhibitors of MAO-A are effective in the therapy of depression, while selective MAO-B inhibitors have been applied alone or in combination to treat Parkinson's and Alzheimer's diseases.[13,14] Thus, the development of specific MAO-B inhibitors could lead to clinically useful neurological disorder therapeutic drugs.

To search for novel MAO-B inhibitors, a variety of benzyloxy substituted molecules have been developed as promising scaffolds with inhibitory activities in the nanomolar range (Fig. 1).[15–25] These MAO-B inhibitors are related to natural compounds such as coumarins, indoles, chromones, chromanones, *a*-tetralone and phthalide analogues. In a recent study, Petzer and colleagues have disclosed that substituted 2-acetylphenols were promising leads for the design of MAO-B inhibitors.[24] Because the structural features of these MAO-B inhibitors with benzyloxy substituents are substantially similar, we explored the probability

State Key Laboratory of Natural Medicines, Department of Natural Medicinal Chemistry, China Pharmaceutical University, 24 Tong Jia Xiang, Nanjing 210009, People's Republic of China. E-mail: cpu_lykong@126.com, xbwang@cpu.edu.cn; Fax: +86 25 8327 1405; Tel: +86 25 8327 1405

† Electronic supplementary information (ESI) available. See DOI: 10.1039/c5md00357a

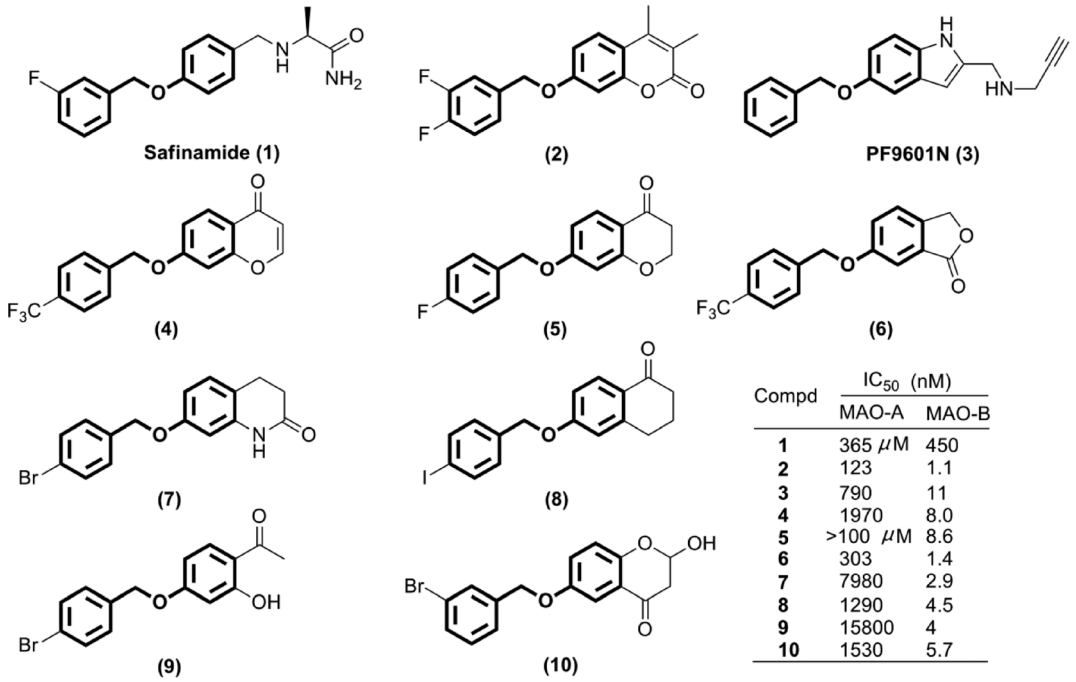

Compd	IC_{50} (nM)	
	MAO-A	MAO-B
1	365 μM	450
2	123	1.1
3	790	11
4	1970	8.0
5	>100 μM	8.6
6	303	1.4
7	7980	2.9
8	1290	4.5
9	15800	4
10	1530	5.7

Fig. 1 Structures of some known MAO inhibitors.

that the simplified acetophenones may also have potential MAO-B inhibitory properties (Fig. 2). In order to obtain the small molecule MAO-B inhibitors, our work was focused on modifying the molecular structure of the potent MAO-B inhibitors by introducing different benzyloxy substituents at C3 and C4 of the acetophenone ring. To further examine the structure–activity relationships (SAR) against MAO-B, different substitutions (F, Cl, Br, CH_3, NO_2 and CF_3) were introduced to the benzyloxy ring, and the properties on MAO-A and MAO-B inhibition were examined.

Results and discussion

Chemistry

The acetophenone derivatives (**1a–1u** and **2a–2m**) were efficiently synthesized using the pathway shown in Scheme 1.

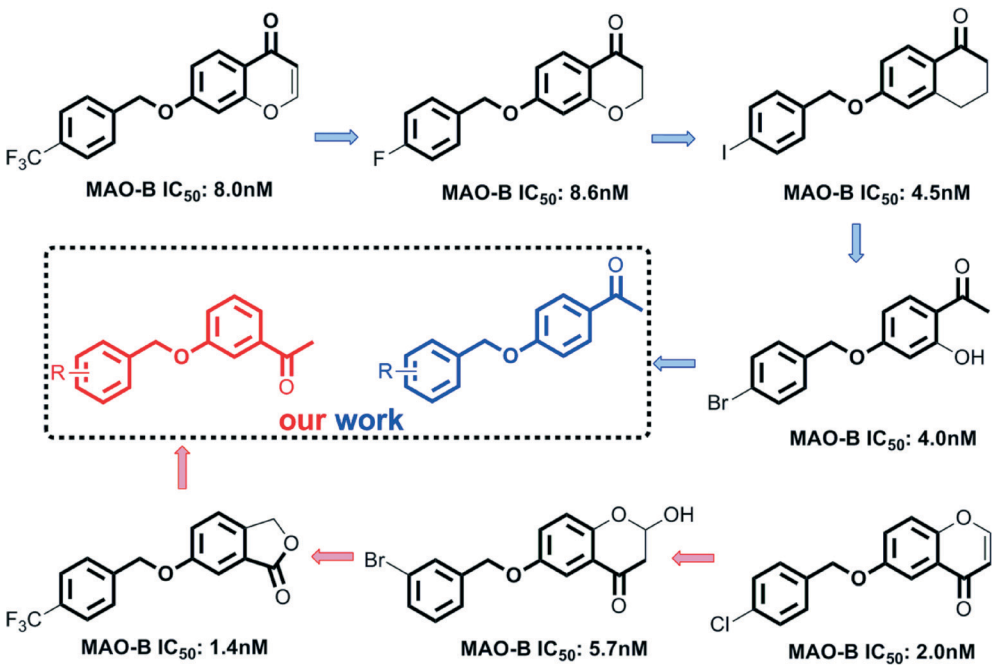

Fig. 2 Design strategy for the novel series of acetophenone derivatives as MAO-B inhibitors.

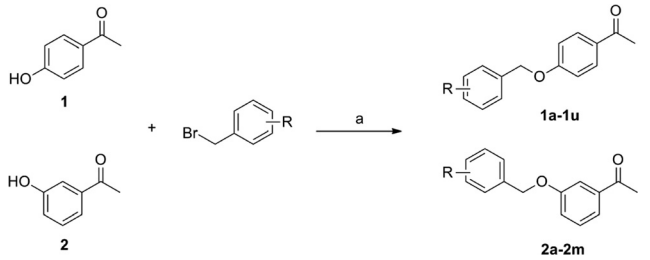

Scheme 1 Syntheses of acetophenone derivatives **1a–1u** and **2a–2m**. Reagents and conditions: (a) K_2CO_3, CH_3CN, reflux, 8 h.

The commercially available starting materials 4-hydroxyacetophenone (**1**) and 3-hydroxyacetophenone (**2**) were reacted with appropriate amounts of benzyl bromide in the presence of K_2CO_3 to give the target compounds in good yields. All compounds were purified by column chromatography. The structures of the compounds were verified by ^{1}H NMR, ^{13}C NMR and mass spectrometry as cited in the experimental section.

Inhibition of MAO activity

The MAO inhibitory activities of compounds **1a–1u** and **2a–2m** were explored by measuring the effects on the production of hydrogen peroxide from *p*-tyramine, according to the reported Amplex Red MAO assay,[26] with iproniazid as a reference. Human MAO-A and MAO-B were purchased from Sigma-Aldrich. Briefly, 0.1 mL of sodium phosphate buffer (0.05 mM, pH 7.4) containing the test drugs at various concentrations and adequate amounts of recombinant MAO-A or MAO-B required and adjusted to obtain, under our experimental conditions, the same reaction velocity, *i.e.*, to oxidize (in the control group) the same concentration of substrate, 165 pmol of *p*-tyramine per min (MAO-A: 1.1 μg protein; specific activity: 150 nmol of *p*-tyramine oxidized to *p*-hydroxyphenylacetaldehyde per min per mg of protein; MAO-B: 7.5 μg protein; specific activity: 22 nmol of *p*-tyramine transformed per min per mg of protein), were incubated for 15 min at 37 °C in a flat-black-bottom 96-well microtest plate placed in a dark fluorimeter chamber. After this incubation period, the reaction was started by adding 200 μM (final concentration) Amplex Red reagent, 1 U per mL of horseradish peroxidase, and 1 mM *p*-tyramine. The production of H_2O_2, and consequently, of resorufin, was quantified at 37 °C using a SpectraMax Paradigm (Molecular Devices, Sunnyvale, CA) multi-mode detection platform reader based on the fluorescence generated (excitation, 545 nm; emission, 590 nm). The specific fluorescence emission was calculated after subtraction of the background activity. The background activity was determined from wells containing all components except the MAO isoforms, which were replaced by a sodium phosphate buffer solution (0.05 mM, pH 7.4). The percent inhibition was calculated by the following expression: (1 − IFi/IFc) × 100% in which IFi and IFc are the fluorescence intensities obtained for MAOs in the presence and absence of inhibitors after subtracting the respective background.

The corresponding IC_{50} values and MAO-B selectivity ratios are shown in Table 1. Based on the screening data, it could be seen that most of the tested compounds were selective inhibitors toward MAO-B with IC_{50} values in the nanomolar range. MAO-A inhibition was very weak, and no apparent structure–activity relationship existed. Among the two series of synthesized compounds, **1j** and **2e** were the most potent inhibitors against MAO-B (**1j**, IC_{50} = 12.9 nM, SI > 7752; **2e**, IC_{50} = 11.7 nM, SI = 3393), being about 623-fold and 687-fold more active than iproniazid.

Initially, to introduce benzyloxy substitution at C4 and C3 of 4-hydroxyacetophenone (**1**) and 3-hydroxyacetophenone (**2**), respectively, compounds **1a** and **2a** were synthesized. As shown in Table 1, the 4-benzyloxy acetophenone **1a** exhibited an IC_{50} value of 110 nM for MAO-B which was more active than the 3-benzyloxy acetophenone **2a** (IC_{50} = 1.95 μM for MAO-B). From this result, it might be concluded that the benzyloxy substitution at C4 of acetophenone was more suitable for volume of the substrate/inhibitor binding pockets than that of 3-benzyloxy acetophenone. Then, we thought of introducing substituents with varying positions and electronic properties to benzyloxy substitution to study the possible effects on MAO-B inhibition potency. It is noteworthy that the benzyloxy acetophenones substituted at the *meta* and *para* positions were more potent than the corresponding *ortho* position (**1e**, **1h**, **1n** and **1q**) and unsubstituted (**1a**) derivatives. Compounds **1h–1p** and **1t–1u** are both bearing halogens (electron-withdrawing groups) which exhibited relatively large enhancement of MAO-B inhibition. However, **1b–1d** substituted with methyl (electron-donating group) showed a slight decrease in MAO-B inhibition. Furthermore, interestingly, compounds with trifluoromethyl substitution (**1q–1s**) of the benzyloxy phenyl ring were more potent for MAO-B inhibition than those with nitrile substitution (**1e–1g**).

Moreover, to introduce benzyloxy substituents to the 3-position of acetophenone to study the possible effects on MAO inhibition, compounds **2a–2m** were synthesized. Compared to compounds **2b–2g** (halogen substitution), the same behaviors were observed for the apparent increase in MAO-B inhibition. Additionally, methyl- and nitrile-substituted benzyloxy acetophenones (**2h–2i** and **2l–2m**) were associated with a slight decrease in MAO-B inhibition potency.

Overall, these results demonstrate that substitution with a wide variety of benzyloxy side chains at C4 and C3 of acetophenone led to structures with potent MAO-B inhibition activity. In contrast, these derivatives were relatively weak MAO-A inhibitors. No clear SAR trend can be obtained from the data, but it seems that compounds (**1f**, **1n–1p**, **2d–2e** and **2m**) bearing nitrile and chloro substituents showed a slight increase in MAO-A inhibitory activities. All these results indicated that the simplified benzyloxy acetophenones were potent and selective MAO-B inhibitors.

Reversibility of MAO-B inhibition

MAO-B inhibitors could be classified as irreversible or reversible because of the different interactions between the

Table 1 MAO inhibitory activities of the synthesized compounds

Compounds	R	MAO-A inhibition[a] (%)	MAO-B IC_{50}[b] (nM)	Selectivity index[c]
1	—	9.74	15.4%[a]	—
2	—	7.18	11.2%	—
1a	H-	8.19	110 ± 7	>909
1b	2-CH_3-	42.9	77.1 ± 3.4	>1297
1c	3-CH_3-	32.3	86.3 ± 6.0	>1159
1d	4-CH_3-	5.96	102 ± 5	>980
1e	2-NO_2-	34	284 ± 30	>352
1f	3-NO_2-	51.3 ± 2.9 μM	104 ± 7	493
1g	4-NO_2-	33.8	96.5 ± 4.6	>1036
1h	2-F-	47.1	56.9 ± 1.3	>1757
1i	3-F-	48.4	83.1 ± 2.4	>1203
1j	4-F-	43.5	12.9 ± 0.8	>7752
1k	2, 4-F-	45.7	27.3 ± 1.6	>3663
1l	3, 4-F-	78.3 ± 4.7 μM	67.9 ± 3.2	1153
1m	3, 4, 5-F-	44.3	84.1 ± 5.8	>1189
1n	2-Cl-	89.6 ± 9.3 μM	311 ± 25	288
1o	3-Cl-	83.3 ± 7.9 μM	21.5 ± 1.6	3874
1p	4-Cl-	93.6 ± 6.4 μM	63.2 ± 3.1	1481
1q	2-CF_3-	70.5 ± 3.3 μM	183 ± 16	385
1r	3-CF_3-	48.9	58.2 ± 1.7	>1718
1s	4-CF_3-	26.4	77.8 ± 7.2	>1285
1t	3-Br-	48.3	214 ± 12	>467
1u	4-Br-	23.2	85.6 ± 4.9	>1168
2a	H-	31.0	1.95 ± 0.17 μM	>51.3
2b	3-F-	31	193 ± 11	>518
2c	4-F-	49.6	86.4 ± 3.7	>1157
2d	3-Cl-	46.8 ± 3.9 μM	34.2 ± 1.6	1368
2e	4-Cl-	39.7 ± 2.1 μM	11.7 ± 0.4	3393
2f	3-Br-	49.1	96.3 ± 6.7	>1038
2g	4-Br-	48.7 ± 1.8 μM	16.5 ± 1.5	2952
2h	3-CH_3-	31.1	893 ± 32	>112
2i	4-CH_3-	23.0	140 ± 8	>714
2j	3-CF_3-	46.7	21.2 ± 0.7	>4717
2k	4-CF_3-	27.2	43.2 ± 1.8	>2315
2l	3-NO_2-	17.8	114 ± 10	>877
2m	4-NO_2-	88.3 ± 7.4 μM	75.4 ± 4.9	1179
Selegiline	—	81.5 ± 6.9 μM	35.6 ± 2.1	2289
Clorgyline	—	7.31 ± 1.07 nM	71.5 ± 8.3 μM	<0.0001
Iproniazid	—	6.18 ± 0.15 μM	8.04 ± 0.46 μM	0.77

[a] The test concentration is 100 μM. [b] IC_{50}: 50% inhibitory concentration (means ± SEM of three experiments). [c] Selectivity index = IC_{50} (MAO-A)/IC_{50} (MAO-B).

inhibitors and the enzyme. As we know, irreversible MAO-B inhibitors may display pharmacological side effects and safety issues. For example, the side effects of selegiline, which is induced by its amphetamine metabolites, are the major drawbacks.[27] Compared to irreversible MAO-B inhibitors, the enzyme activity of reversible MAO-B inhibitors can be recovered when the inhibitors are metabolized. Moreover, the enzyme activity will decrease when the substrate concentration increases. For these reasons, discovering novel reversible MAO-B inhibitors may be valuable.

To evaluate whether the benzyloxy-substituted acetophenone derivatives were reversible or irreversible MAO-B inhibitors, the time dependencies of inhibition were evaluated.[28] Compounds **1j** and **2e** were selected as representative inhibitors since they displayed the most potent MAO-B inhibitory activities. Pargyline, a known irreversible MAO-B inhibitor, was used as a reference compound. For a reversible inhibitor, the MAO-B activity would almost be same, when the enzyme is pre-incubated with a reversible inhibitor over different time periods. In contrast, when the enzyme is pre-incubated with an irreversible inhibitor (pargyline) over different time periods, the MAO-B activity would show a time-dependent reduction. Compounds **1j** and **2e** were pre-incubated with MAO-B over different time periods (0–60 min) at a concentration of about two fold IC_{50}. As shown in Fig. 3, we could observe a slight increase in catalytic activities when **1j** and **2e** were pre-incubated with MAO-B, and the results demonstrated that **1j** and **2e** were not time-dependent MAO-B inhibitors. In contrast, treatment of MAO-B with pargyline led to a time-dependent reduction in enzyme activity. These experiments clearly indicated that the acetophenone derivatives were reversible MAO-B inhibitors.

Kinetic study of MAO-B inhibition

Compounds **1j** and **2e** were also used to further investigate the mode of MAO-B inhibition. The type of MAO-B inhibition

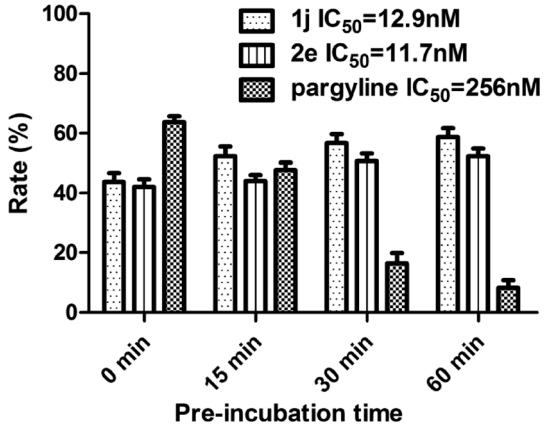

Fig. 3 The time-dependent inhibition of MAO-B by compounds **1j** and **2e** and pargyline. All compounds were pre-incubated for various periods of time (0–60 min) with MAO-B at concentrations equal to two-fold the IC_{50} values for the inhibition of the enzyme. After dilution to concentrations equal to the IC_{50}, the inhibitory rates were recorded.

was determined by Michaelis–Menten kinetic experiments.[29] The catalytic rates were measured at five different *p*-tyramine concentrations (50–500 μM), and each plot was constructed at four different concentrations of **1j** (0, 6, 12 and 25 nM) and **2e** (0, 5, 10 and 20 nM). The overlaid reciprocal Lineweaver–Burk plots (Fig. 4) showed that the plots for different concentrations of **1j** and **2e** were linear and intersected at the *y*-axis. This pattern indicated that **1j** and **2e** were competitive MAO-B inhibitors, and these results further proved that the acetophenone derivatives were reversible MAO-B inhibitors.

Molecular modeling study

In order to explain the binding modes of compounds **1j** and **2e**, the molecular docking study was performed using software package MOE 2008.10.[30] The X-ray crystal structures of the hMAO-A (PDB 2Z5X) and hMAO-B (PDB 2V61) were applied to build the starting model, which were obtained from the Protein Data Bank (www.rcsb.org).[31,32] Heteroatoms and water molecules in the PDB files were removed, and all hydrogen atoms were subsequently added to the proteins. According to the inhibition results, compounds **1j** and **2e** were selected as typical ligands. Compounds **1j** and **2e** were drawn and then protonated using the protonate 3D protocol, and energy was minimized using the MMFF94x force field in MOE. When the enzymes and compounds were ready for the docking study, **1j** and **2e** were docked into the active site of the protein by the "Triangle Matcher" method. The Dock scoring in MOE software was performed using the ASE scoring function and force field was selected as the refinement method. The best 10 poses of molecules were retained and scored. After docking, the geometry of the resulting complex was studied using MOE's pose viewer utility.

The 3D and 2D binding pictures are illustrated in Fig. 5. As shown in Fig. 5A and B, compound **1j** is located in the well-known binding pocket of MAO-B,[11] with the F-substituted benzyl positioned at the bottom of the substrate cavity. There was a π–π interaction formed between the benzyloxy ring of the ligand (**1j**) and Tyr 398. In addition, the acetophenone ring occupied the entrance cavity, which was a hydrophobic subpocket existing only in the MAO-B isoform and consisted of Leu 171, Ile 199, Tyr 326, Ile 316, Phe 99, Pro 104 and Phe 168. Surprisingly, different interactions between the ligand (**2e**) and MAO-B were observed in Fig. 5C and D. A hydrogen bond formed between the carbonyl oxygen of the ligand and Tyr 435-OH, and the acetophenone moiety occupied the substrate cavity. However, no direct interaction between the ligands (**1j** and **2e**) and the MAO-A (PDB code 2Z5X) was observed in Fig. S1A–D (ESI†).

Prediction of BBB penetration of the compounds

With the aim of developing CNS drugs, the ability of compounds to cross the blood–brain barrier (BBB) plays an important role. So in the drug discovery process, BBB permeability properties should be determined as early as possible.[33] To cross the BBB, molecules should meet the limiting terms of Lipinski's rules:[34] molecular weight (MW) less than 500, the number of hydrogen bond donor atoms (HBD) less than 5, the number of hydrogen bond acceptor atoms (HBA) less than 10, the calculated logarithm of the octanol–water

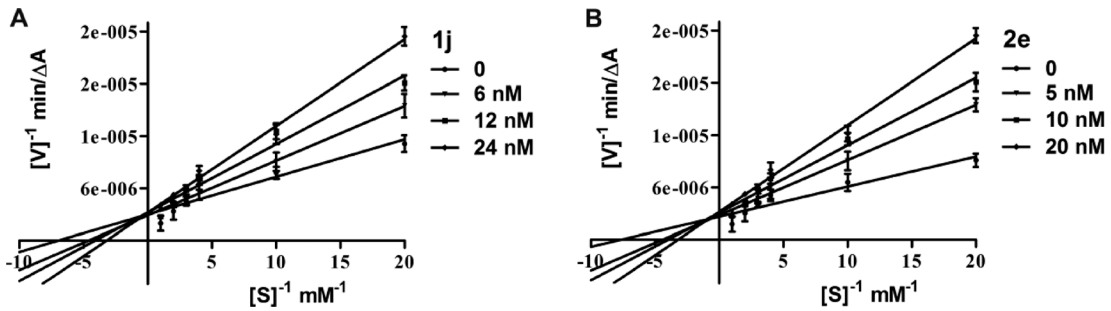

Fig. 4 Kinetic study on the mechanism of MAO-B inhibition by compounds **1j** (A) and **2e** (B). The overlaid Lineweaver–Burk reciprocal plots of MAO-B initial velocity at increasing substrate concentration (50–500 μM) in the absence of an inhibitor and in the presence of **1j** (A) and **2e** (B) are shown. The lines were derived from a weighted least-squares analysis of the data points.

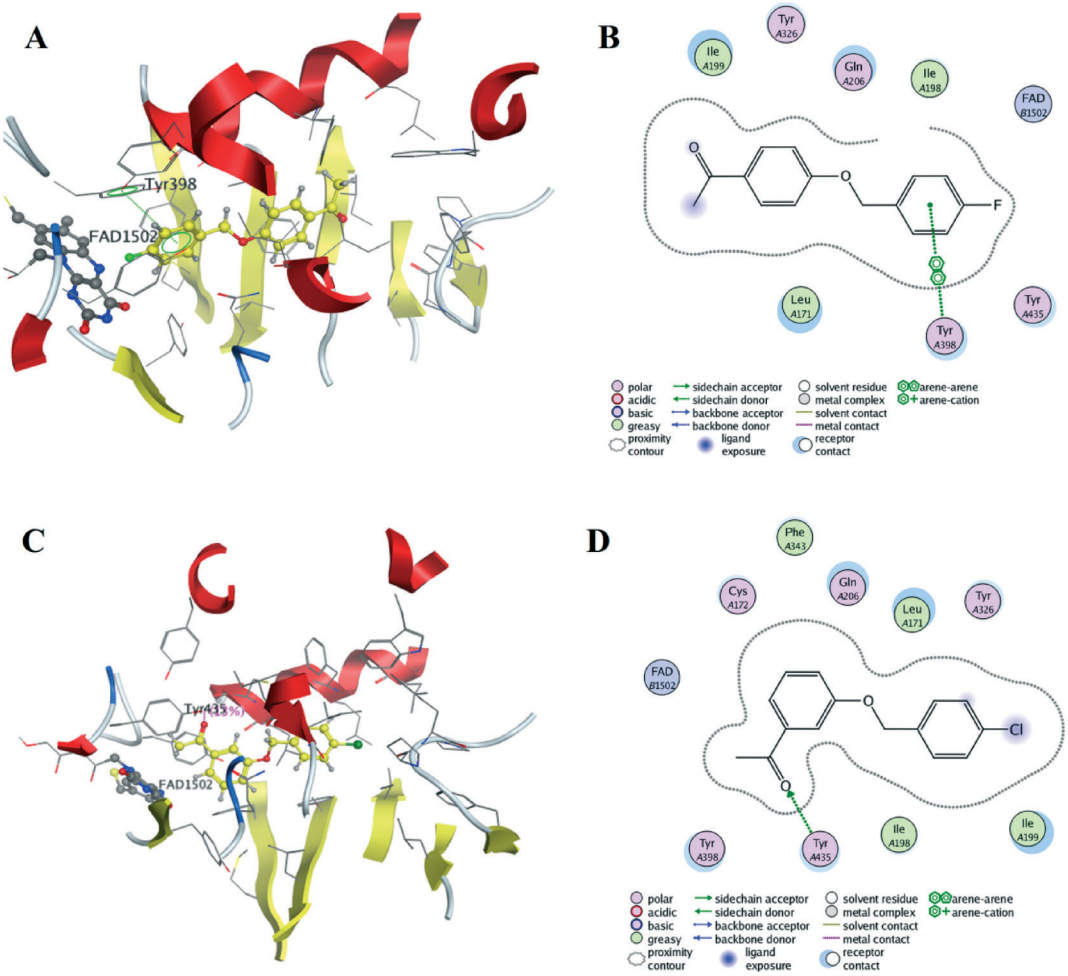

Fig. 5 (A) 3D docking model of compound **1j** with MAO-B. Atom colors: yellow—carbon atoms of **1j**, gray—carbon atoms of residues of MAO-B, dark blue—halogen atoms, red—oxygen atoms. The dashed lines represent the interactions between the protein and the ligand. (B) 2D schematic diagram of the docking model of compound **1j** with MAO-B. (C) 3D docking model of compound **2e** with MAO-B. (D) 2D schematic diagram of the docking model of compound **2e** with MAO-B. The figure was prepared using the ligand interaction application in MOE. (For interpretation of the references to color in this figure legend, the reader is referred to the web version of this article.)

partition coefficient (Clog *P*) less than 5, and the small polar surface area less than 90 Å.[2] The log BB is calculated using the following equation: log BB = 0.0148 × PSA + 0.152 × Clog *P* + 0.130.[22] Calculated log BB (Tables 2 and S1 ESI†) for potential applications in the brain and defined by the restrictive terms of Lipinski's rules, and all compounds satisfied the possible brain penetration and drug-like properties.

Cell toxicity

Based on the results above, compounds **1j** and **2e** as the most potent and selective inhibitors against MAO-B were selected to further investigate the potential toxicity effect on SH-SY5Y cells.[35] After incubating the cells with compounds **1j** and **2e** for 48 h, the cell viability was determined by the 3-(4,5-dimethylthiazol-2-yl)-2,5-diphenyltetrazolium (MTT) assay. As shown in Fig. 6, the results revealed that compounds **1j** and **2e** at 3–50 μM did not have neurotoxicity. This suggested that compounds **1j** and **2e** might be used to develop promising drug candidates for the therapy of neurodegenerative diseases.

Conclusions

In this work, two series of benzyloxy-substituted acetophenone derivatives were designed, synthesized and evaluated for MAO inhibitory activity *in vitro*. It was observed that most of the studied compounds were remarkably reversible, competitive and selective MAO-B inhibitors with nanomolar inhibitory potency. In particular, compounds **1j** and **2e** were the most potent MAO-B inhibitors. The MAO inhibition data indicated that substitutions at the C3 and C4 positions of the acetophenone moiety, particularly with the halogen substituted benzyloxy, were more favorable for MAO-B inhibition. Molecular docking analysis of compounds **1j** and **2e** suggested that the potent MAO-B inhibition and high selectivity might be ascribed to the π–π and hydrogen bond

Table 2 Physical properties of some representative compounds

Compounds	MW[a]	Clog *P*[a]	HBA[a]	HBD[a]	PAS[a]	Log BB[a]
1a	226.27	3.569	2	0	26.3	0.292248
1d	240.3	4.068	2	0	26.3	0.368096
1g	271.27	3.312	4	0	78.11	−0.513604
1j	244.26	3.712	3	0	26.3	0.313984
1k	262.25	3.855	4	0	26.3	0.33572
1l	262.25	3.785	4	0	26.3	0.32508
1m	280.24	3.858	5	0	26.3	0.336176
1p	260.72	4.282	3	0	26.3	0.400624
1s	294.27	4.452	5	0	26.3	0.426464
1u	305.17	4.432	3	0	26.3	0.423424
2a	226.27	3.569	2	0	26.3	0.292248
2c	244.26	3.712	3	0	26.3	0.313984
2e	260.72	4.282	3	0	26.3	0.400624
2g	305.17	4.432	3	0	26.3	0.423424
2i	240.3	4.068	2	0	26.3	0.368096
2k	294.27	4.452	5	0	26.3	0.426464
2m	271.27	3.312	4	0	78.11	−0.513604
Rules	≤450	≤5.0	≤10	≤5	≤90	≥−1.0

[a] MW: molecular weight; Clog *P*: calculated logarithm of the octanol–water partition coefficient; HBA: hydrogen-bond acceptor atoms; HBD: hydrogen-bond donor atoms; PSA: polar surface area; log BB = 0.0148 × PSA + 0.152 × Clog *P* + 0.130.

interactions and the larger set of residues interacting with MAO-B, respectively. Finally, due to the possible BBB permeability and low neurotoxicity in SH-SY5Y cells, these compounds could be used to develop promising drug candidates for the therapy of neurodegenerative diseases.

Experimental

General

All common reagents and solvents were obtained from commercial suppliers and used without further purification. The reaction progress was monitored using analytical thin layer chromatography (TLC) on precoated silica gel GF254 plates (Qingdao Haiyang Chemical Plant, Qingdao, China), and the spots were detected under UV light (254 nm). Column chromatography was performed on silica gel (90–150 μm; Qingdao Marine Chemical Inc.) Melting point was measured using an XT-4 micromelting point instrument and uncorrected. ^{1}H NMR and ^{13}C NMR spectra were measured using a Bruker ACF-500 spectrometer at 25 °C and referenced to TMS. Chemical shifts are reported in ppm (δ) using the residual solvent line as internal standard. Mass spectra were obtained using an MS Agilent 1100 Series LC/MSD Trap mass spectrometer (ESI-MS) and a Mariner ESI-TOF spectrometer (HRESI-MS), respectively.

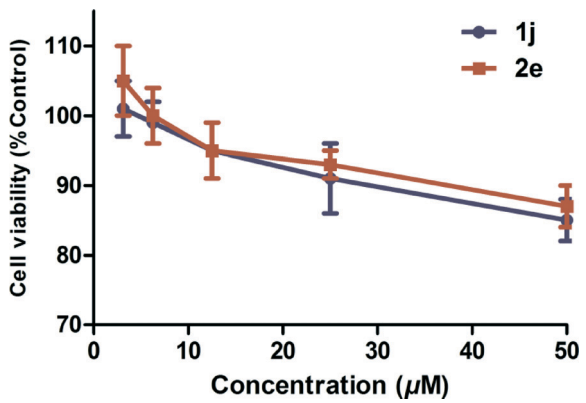

Fig. 6 The cell viability of compounds **1j** and **2e** in SH-SY5Y cells at 3.125–50 μM.

General procedure for the preparation of acetophenone derivatives (1a–1u)[36,37]

1-(4-Hydroxyphenyl)ethanone (1.0 mmol) was suspended in acetonitrile (20 mL) containing K_2CO_3 (2.0 mmol). The reaction was treated with appropriately substituted arylalkyl bromide (1.2 mmol) and heated under reflux for 8 h. The reaction progress was monitored using silica gel TLC with petroleum ether/ethyl acetate as the mobile phase. Upon completion, the acetonitrile was evaporated *in vacuo* and the mixture was then poured into water, which was extracted with 3 × 100 mL of EtOAc, washed with brine, dried over anhydrous Na_2SO_4 and purified by chromatography (PE/EA) on silica gel.

1-(4-(Benzyloxy)phenyl)ethanone (1a)

Yield 92%, white solid, m.p. 92–94 °C; ^{1}H NMR (500 MHz, DMSO) δ 7.95 (d, J = 8.8 Hz, 2H), 7.48 (d, J = 7.2 Hz, 2H), 7.42 (t, J = 7.4 Hz, 2H), 7.37 (d, J = 7.2 Hz, 1H), 7.14 (d, J = 8.8 Hz, 2H), 5.23 (s, 2H), 2.53 (s, 3H); ^{13}C NMR (126 MHz, DMSO) δ 196.71, 162.67, 137.01, 130.93, 130.62, 130.62, 128.96, 128.96, 128.46, 128.21, 128.21, 115.16, 115.16, 70.02, 26.84. ESI-MS m/z: 226.9 $[M + H]^+$; HRMS (ESI) m/z 227.1066 $[M + H]^+$ (calcd for 227.1067, $C_{15}H_{15}O_2$).

1-(4-((2-Methylbenzyl)oxy)phenyl)ethanone (1b)

Yield 90%, white solid, m.p. 97–99 °C; ^{1}H NMR (500 MHz, DMSO) δ 7.96 (d, J = 8.8 Hz, 2H), 7.44 (d, J = 7.4 Hz, 1H),

7.32–7.19 (m, 3H), 7.16 (d, J = 8.8 Hz, 2H), 5.21 (s, 2H), 2.54 (s, 3H), 2.35 (s, 3H); ^{13}C NMR (126 MHz, DMSO) δ 196.72, 162.80, 137.14, 134.90, 130.94, 130.94, 130.69, 130.65, 129.07, 128.71, 126.30, 115.10, 115.10, 68.78, 26.85, 18.92. ESI-MS m/z: 240.9 $[M + H]^+$; HRMS (ESI) m/z 241.1225 $[M + H]^+$ (calcd for 241.1223, $C_{16}H_{17}O_2$).

1-(4-((3-Methylbenzyl)oxy)phenyl)ethanone (1c)

Yield 85%, white solid, m.p. 70–72 °C; ^{1}H NMR (500 MHz, DMSO) δ 7.95 (d, J = 8.8 Hz, 2H), 7.34–7.24 (m, 3H), 7.17 (d, J = 7.2 Hz, 1H), 7.13 (d, J = 8.8 Hz, 2H), 5.18 (s, 2H), 2.53 (s, 3H), 2.34 (s, 3H); ^{13}C NMR (126 MHz, DMSO) δ 196.71, 162.72, 138.16, 136.92, 130.93, 130.93, 130.60, 129.10, 128.87, 128.76, 125.30, 115.13, 115.13, 70.06, 26.84, 21.44. ESI-MS m/z: 240.9 $[M + H]^+$; HRMS (ESI) m/z 241.1222 $[M + H]^+$ (calcd for 241.1223, $C_{16}H_{17}O_2$).

1-(4-((4-Methylbenzyl)oxy)phenyl)ethanone (1d)

Yield 88%, white solid, m.p. 100–102 °C; ^{1}H NMR (500 MHz, DMSO) δ 7.94 (d, J = 8.7 Hz, 2H), 7.36 (d, J = 7.8 Hz, 2H), 7.22 (d, J = 7.7 Hz, 2H), 7.12 (d, J = 8.7 Hz, 2H), 5.17 (s, 2H), 2.53 (s, 3H), 2.33 (s, 3H); ^{13}C NMR (126 MHz, DMSO) δ 196.68, 162.69, 137.74, 133.95, 130.89, 130.89, 130.53, 129.50, 129.50, 128.30, 128.30, 115.15, 115.15, 69.92, 26.83, 21.23. ESI-MS m/z: 240.9 $[M + H]^+$; HRMS (ESI) m/z 241.1224 $[M + H]^+$ (calcd for 241.1223, $C_{16}H_{17}O_2$).

1-(4-((2-Nitrobenzyl)oxy)phenyl)ethanone (1e)

Yield 90%, white solid, m.p. 120–122 °C; ^{1}H NMR (500 MHz, DMSO) δ 8.16 (d, J = 8.0 Hz, 1H), 7.96 (d, J = 8.9 Hz, 2H), 7.87–7.78 (m, 2H), 7.66 (ddd, J = 8.5, 5.5, 3.5 Hz, 1H), 7.15 (d, J = 8.9 Hz, 2H), 5.59 (s, 2H), 2.54 (s, 3H); ^{13}C NMR (126 MHz, DMSO) δ 196.74, 162.13, 148.04, 134.49, 132.33, 131.03, 131.00, 131.00, 129.83, 129.80, 125.35, 115.12, 115.12, 67.10, 26.88. ESI-MS m/z: 271.9 $[M + H]^+$; HRMS (ESI) m/z 272.0919 $[M + H]^+$ (calcd for 272.0917, $C_{15}H_{14}NO_4$).

1-(4-((3-Nitrobenzyl)oxy)phenyl)ethanone (1f)

Yield 91%, white solid, m.p. 106–108 °C; ^{1}H NMR (500 MHz, DMSO) δ 8.35 (s, 1H), 8.23 (d, J = 8.1 Hz, 1H), 7.96 (t, J = 8.7 Hz, 3H), 7.74 (t, J = 7.9 Hz, 1H), 7.17 (d, J = 8.8 Hz, 2H), 5.40 (s, 2H), 2.54 (s, 3H); ^{13}C NMR (126 MHz, DMSO) δ 196.73, 162.22, 148.39, 139.42, 134.55, 130.98, 130.98, 130.90, 130.60, 123.33, 122.55, 115.19, 115.19, 68.69, 26.86. ESI-MS m/z: 271.9 $[M + H]^+$; HRMS (ESI) m/z 272.0919 $[M + H]^+$ (calcd for 272.0916, $C_{15}H_{14}NO_4$).

1-(4-((4-Nitrobenzyl)oxy)phenyl)ethanone (1g)

Yield 85%, white solid, m.p. 125–127 °C; ^{1}H NMR (500 MHz, DMSO) δ 8.28 (d, J = 8.6 Hz, 2H), 7.96 (d, J = 8.8 Hz, 2H), 7.75 (d, J = 8.5 Hz, 2H), 7.16 (d, J = 8.8 Hz, 2H), 5.41 (s, 2H), 2.54 (s, 3H); ^{13}C NMR (126 MHz, DMSO) δ 196.74, 162.20, 147.64, 144.89, 130.98, 130.98, 130.95, 128.78, 128.78, 124.11, 124.11, 115.20, 115.20, 68.79, 26.86. ESI-MS m/z: 271.9 $[M + H]^+$; HRMS (ESI) m/z 272.0918 $[M + H]^+$ (calcd for 272.0917, $C_{15}H_{14}NO_4$).

1-(4-((2-Fluorobenzyl)oxy)phenyl)ethanone (1h)

Yield 87%, white solid, m.p. 87–88 °C; ^{1}H NMR (500 MHz, DMSO) δ 7.96 (d, J = 8.8 Hz, 2H), 7.59 (t, J = 7.5 Hz, 1H), 7.46 (td, J = 7.4, 1.6 Hz, 1H), 7.36–7.22 (m, 2H), 7.16 (d, J = 8.8 Hz, 2H), 5.27 (s, 2H), 2.54 (s, 3H); ^{13}C NMR (126 MHz, DMSO) δ 196.74, 162.47, 131.25, 131.22, 131.11, 131.05, 130.96, 130.80, 125.07, 125.04, 116.01, 115.85, 115.06, 60.21, 26.87. ESI-MS m/z: 244.9 $[M + H]^+$; HRMS (ESI) m/z 245.0973 $[M + H]^+$ (calcd for 245.0974, $C_{15}H_{14}FO_2$).

1-(4-((3-Fluorobenzyl)oxy)phenyl)ethanone (1i)

Yield 83%, white solid, m.p. 82–83 °C; ^{1}H NMR (500 MHz, DMSO) δ 7.96 (d, J = 8.8 Hz, 2H), 7.47 (dd, J = 14.1, 8.0 Hz, 1H), 7.32 (dd, J = 8.0, 4.5 Hz, 2H), 7.19 (td, J = 8.7, 2.1 Hz, 1H), 7.14 (d, J = 8.8 Hz, 2H), 5.26 (s, 2H), 2.53 (s, 3H); ^{13}C NMR (126 MHz, DMSO) δ 196.72, 162.42, 139.99, 139.93, 131.04, 130.98, 130.94, 130.78, 124.03, 124.01, 115.28, 115.17, 114.84, 69.13, 26.84. ESI-MS m/z: 244.9 $[M + H]^+$; HRMS (ESI) m/z 245.0971 $[M + H]^+$ (calcd for 245.0972, $C_{15}H_{14}FO_2$).

1-(4-((4-Fluorobenzyl)oxy)phenyl)ethanone (1j)

Yield 83%, white solid, m.p. 75–77 °C; ^{1}H NMR (500 MHz, DMSO) δ 7.95 (d, J = 8.8 Hz, 2H), 7.54 (dd, J = 8.4, 5.7 Hz, 2H), 7.25 (t, J = 8.8 Hz, 2H), 7.13 (d, J = 8.8 Hz, 2H), 5.21 (s, 2H), 2.53 (s, 3H); ^{13}C NMR (126 MHz, DMSO) δ 196.72, 162.56, 161.39, 133.26, 130.93, 130.93, 130.68, 130.54, 130.48, 115.87, 115.70, 115.15, 115.15, 69.29, 26.84. ESI-MS m/z: 244.9 $[M + H]^+$; HRMS (ESI) m/z 245.0970 $[M + H]^+$ (calcd for 245.0972, $C_{15}H_{14}FO_2$).

1-(4-((2,4-Difluorobenzyl)oxy)phenyl)ethanone (1k)

Yield 87%, white solid, m.p. 66–68 °C; ^{1}H NMR (500 MHz, DMSO) δ 7.96 (d, J = 8.8 Hz, 2H), 7.66 (dd, J = 15.3, 8.5 Hz, 1H), 7.33 (td, J = 10.4, 2.2 Hz, 1H), 7.22–7.09 (m, 3H), 5.23 (s, 2H), 2.54 (s, 3H); ^{13}C NMR (126 MHz, DMSO) δ 196.73, 163.87, 162.38, 160.24, 132.71, 130.94, 130.86, 115.06, 115.06, 112.18, 104.77, 104.57, 104.36, 63.92, 26.84. ESI-MS m/z: 262.9 $[M + H]^+$; HRMS (ESI) m/z 263.0880 $[M + H]^+$ (calcd for 263.0878, $C_{15}H_{13}F_2O_2$).

1-(4-((3,4-Difluorobenzyl)oxy)phenyl)ethanone (1l)

Yield 85%, white solid, m.p. 61–63 °C; ^{1}H NMR (500 MHz, DMSO) δ 7.96 (d, J = 8.8 Hz, 2H), 7.57 (dd, J = 14.2, 5.2 Hz, 1H), 7.52–7.42 (m, 1H), 7.35 (dd, J = 7.0, 5.3 Hz, 1H), 7.13 (d, J = 8.8 Hz, 2H), 5.21 (s, 2H), 2.53 (s, 3H); ^{13}C NMR (126 MHz, DMSO) δ 196.71, 162.33, 134.80, 130.93, 130.93, 130.81, 125.08, 118.11, 117.98, 117.40, 117.26, 115.15, 115.15, 68.68, 26.82. ESI-MS m/z: 262.9 $[M + H]^+$; HRMS (ESI) m/z 263.0877 $[M + H]^+$ (calcd for 263.0878, $C_{15}H_{13}F_2O_2$).

1-(4-((3,4,5-Trifluorobenzyl)oxy)phenyl)ethanone (1m)

Yield 90%, white solid, m.p. 80–82 °C; ^{1}H NMR (500 MHz, DMSO) δ 7.96 (d, J = 8.9 Hz, 2H), 7.53–7.39 (m, 2H), 7.14 (d, J = 8.9 Hz, 2H), 5.21 (s, 2H), 2.54 (s, 3H); ^{13}C NMR (126 MHz, DMSO) δ 196.73, 162.10, 151.71, 139.51, 134.05, 130.95, 130.95, 115.17, 115.17, 112.81, 112.77, 112.68, 112.64, 68.27, 26.84. ESI-MS m/z: 280.9 $[M + H]^+$; HRMS (ESI) m/z 281.0786 $[M + H]^+$ (calcd for 281.0784, $C_{15}H_{12}F_3O_2$).

1-(4-((2-Chlorobenzyl)oxy)phenyl)ethanone (1n)

Yield 83%, white solid, m.p. 94–96 °C; ^{1}H NMR (500 MHz, DMSO) δ 7.97 (d, J = 8.7 Hz, 2H), 7.67–7.60 (m, 1H), 7.55 (dd, J = 8.0, 5.9 Hz, 1H), 7.48–7.37 (m, 2H), 7.16 (d, J = 8.8 Hz, 2H), 5.28 (s, 2H), 2.54 (d, J = 5.0 Hz, 3H); ^{13}C NMR (126 MHz, DMSO) δ 196.74, 162.47, 134.29, 133.24, 130.99, 130.99, 130.86, 130.74, 130.55, 129.95, 127.90, 115.08, 115.08, 67.68, 26.87. ESI-MS m/z: 260.9 $[M + H]^+$; HRMS (ESI) m/z 261.0676 $[M + H]^+$ (calcd for 261.0677, $C_{15}H_{14}ClO_2$).

1-(4-((3-Chlorobenzyl)oxy)phenyl)ethanone (1o)

Yield 89%, white solid, m.p. 79–81 °C; ^{1}H NMR (500 MHz, DMSO) δ 7.96 (d, J = 8.8 Hz, 2H), 7.55 (s, 1H), 7.49–7.39 (m, 3H), 7.14 (d, J = 8.8 Hz, 2H), 5.25 (s, 2H), 2.53 (s, 3H); ^{13}C NMR (126 MHz, DMSO) δ 196.73, 162.39, 139.61, 133.67, 130.95, 130.95, 130.89, 130.78, 128.39, 127.84, 126.69, 115.16, 115.16, 69.05, 26.85. ESI-MS m/z: 260.9 $[M + H]^+$; HRMS (ESI) m/z 261.0679 $[M + H]^+$ (calcd for 261.0677, $C_{15}H_{14}ClO_2$).

1-(4-((4-Chlorobenzyl)oxy)phenyl)ethanone (1p)

Yield 92%, white solid, m.p. 88–89 °C; ^{1}H NMR (500 MHz, DMSO) δ 7.95 (d, J = 8.8 Hz, 2H), 7.50 (q, J = 8.5 Hz, 4H), 7.13 (d, J = 8.8 Hz, 2H), 5.23 (s, 2H), 2.53 (s, 3H); ^{13}C NMR (126 MHz, DMSO) δ 196.72, 162.46, 136.08, 133.09, 130.94, 130.94, 130.73, 130.02, 130.02, 128.98, 128.98, 115.17, 115.17, 69.16, 26.85. ESI-MS m/z: 260.9 $[M + H]^+$; HRMS (ESI) m/z 261.0678 $[M + H]^+$ (calcd for 261.0677, $C_{15}H_{14}ClO_2$).

1-(4-((2-(Trifluoromethyl)benzyl)oxy)phenyl)ethanone (1q)

Yield 94%, white solid, m.p. 68–70 °C; ^{1}H NMR (500 MHz, DMSO) δ 7.97 (d, J = 8.9 Hz, 2H), 7.86–7.71 (m, 3H), 7.62 (t, J = 7.6 Hz, 1H), 7.14 (d, J = 8.9 Hz, 2H), 5.35 (s, 2H), 2.54 (s, 3H); ^{13}C NMR (126 MHz, DMSO) δ 192.11, 159.32, 133.15, 131.74, 129.61, 129.53, 129.53, 129.48, 128.02, 125.48 (q, J = 125.2 Hz), 125.13, 124.13, 114.31, 114.31, 68.60, 30.32. ESI-MS m/z: 294.9 $[M + H]^+$; HRMS (ESI) m/z 295.0939 $[M + H]^+$ (calcd for 295.0940, $C_{16}H_{14}F_3O_2$).

1-(4-((3-(Trifluoromethyl)benzyl)oxy)phenyl)ethanone (1r)

Yield 94%, white solid, m.p. 82–84 °C; ^{1}H NMR (500 MHz, DMSO) δ 7.97 (d, J = 8.8 Hz, 2H), 7.86 (s, 1H), 7.80 (d, J = 7.6 Hz, 1H), 7.73 (d, J = 7.8 Hz, 1H), 7.67 (t, J = 7.7 Hz, 1H), 7.16 (d, J = 8.8 Hz, 2H), 5.34 (s, 2H), 2.54 (s, 3H); ^{13}C NMR (126 MHz, DMSO) δ 196.72, 162.38, 138.57, 132.17, 130.96, 130.96, 130.83, 130.10, 125.18, 125.15, 124.59, 124.56 (q, J = 125.2 Hz), 115.15, 115.15, 69.09, 26.84. ESI-MS m/z: 294.9 $[M + H]^+$; HRMS (ESI) m/z 295.0941 $[M + H]^+$ (calcd for 295.0940, $C_{16}H_{14}F_3O_2$).

1-(4-((4-(Trifluoromethyl)benzyl)oxy)phenyl)ethanone (1s)

Yield 91%, white solid, m.p. 77–79 °C; ^{1}H NMR (500 MHz, DMSO) δ 7.96 (d, J = 8.7 Hz, 2H), 7.78 (d, J = 8.1 Hz, 2H), 7.70 (d, J = 8.0 Hz, 2H), 7.15 (d, J = 8.7 Hz, 2H), 5.35 (s, 2H), 2.53 (s, 3H); ^{13}C NMR (126 MHz, DMSO) δ 196.71, 162.34, 141.89, 130.96, 130.96, 130.85, 129.13, 128.87, 128.51, 128.51, 125.82 (q, J = 125.2 Hz), 123.60, 115.17, 115.17, 69.08, 26.81. ESI-MS m/z: 294.9 $[M + H]^+$; HRMS (ESI) m/z 295.0938 $[M + H]^+$ (calcd for 295.0940, $C_{16}H_{14}F_3O_2$).

1-(4-((3-Bromobenzyl)oxy)phenyl)ethanone (1t)

Yield 84%, white solid, m.p. 81–83 °C; ^{1}H NMR (500 MHz, DMSO) δ 7.96 (d, J = 8.8 Hz, 2H), 7.70 (s, 1H), 7.56 (d, J = 8.0 Hz, 1H), 7.49 (d, J = 7.7 Hz, 1H), 7.39 (t, J = 7.8 Hz, 1H), 7.14 (d, J = 8.8 Hz, 2H), 5.25 (s, 2H), 2.54 (s, 3H); ^{13}C NMR (126 MHz, DMSO) δ 196.74, 162.39, 139.86, 131.30, 131.18, 130.96, 130.96, 130.78, 130.74, 127.10, 122.22, 115.17, 115.17, 68.99, 26.86. ESI-MS m/z: 306.9 $[M + H]^+$; HRMS (ESI) m/z 305.0174 $[M + H]^+$ (calcd for 305.0172, $C_{15}H_{14}BrO_2$).

1-(4-((4-Bromobenzyl)oxy)phenyl)ethanone (1u)

Yield 90%, white solid, m.p. 101–103 °C; ^{1}H NMR (500 MHz, DMSO) δ 7.95 (d, J = 8.9 Hz, 2H), 7.62 (d, J = 8.3 Hz, 2H), 7.45 (d, J = 8.3 Hz, 2H), 7.13 (d, J = 8.8 Hz, 2H), 5.22 (s, 2H), 2.53 (s, 3H); ^{13}C NMR (126 MHz, DMSO) δ 196.71, 162.43, 136.49, 131.89, 131.89, 130.93, 130.93, 130.72, 130.30, 130.30, 121.59, 115.17, 115.17, 69.17, 26.86. ESI-MS m/z: 306.9 $[M + H]^+$; HRMS (ESI) m/z 305.0171 $[M + H]^+$ (calcd for 305.0172, $C_{15}H_{14}BrO_2$).

General procedure for the preparation of acetophenone derivatives (2a–2m)[38]

1-(3-Hydroxyphenyl)ethanone (1.0 mmol) was suspended in acetonitrile (20 mL) containing K_2CO_3 (2.0 mmol). The reaction was treated with appropriately substituted arylalkyl bromide (1.2 mmol) and heated under reflux for 8 h. The reaction progress was monitored using silica gel TLC with petroleum ether/ethyl acetate as the mobile phase. Upon completion, the acetonitrile was evaporated *in vacuo*, and the mixture was then poured into water, which was extracted with 3 × 100 mL of EtOAc, washed with brine, dried over anhydrous Na_2SO_4 and purified by chromatography (PE/EA) on silica gel.

1-(3-(Benzyloxy)phenyl)ethanone (2a)

Yield 95%, colorless oil; ^{1}H NMR (500 MHz, DMSO) δ 7.57 (dd, J = 11.3, 4.9 Hz, 2H), 7.52–7.39 (m, 5H), 7.36 (t, J = 7.3 Hz, 1H), 7.31 (dd, J = 8.2, 1.8 Hz, 1H), 5.20 (s, 2H), 2.59 (s, 3H); ^{13}C NMR (126 MHz, DMSO) δ 198.13, 159.02, 138.81, 137.30, 130.36, 128.93, 128.93, 128.37, 128.18, 128.18, 121.41, 120.39, 114.29, 69.98, 27.28. ESI-MS m/z: 226.8 $[M + H]^+$; HRMS (ESI) m/z 227.1068 $[M + H]^+$ (calcd for 227.1067, $C_{15}H_{15}O_2$).

1-(3-((3-Fluorobenzyl)oxy)phenyl)ethanone (2b)

Yield 95%, colorless oil; ^{1}H NMR (500 MHz, DMSO) δ 7.62–7.54 (m, 2H), 7.47 (dd, J = 15.4, 7.8 Hz, 2H), 7.36–7.28 (m, 3H), 7.18 (td, J = 8.8, 2.3 Hz, 1H), 5.23 (s, 2H), 2.59 (s, 3H); ^{13}C NMR (126 MHz, DMSO) δ 198.11, 158.80, 140.30, 140.24, 138.83, 131.00, 130.94, 130.40, 123.99, 123.97, 121.59, 120.39, 114.28, 69.11, 27.28. ESI-MS m/z: 244.8 $[M + H]^+$; HRMS (ESI) m/z 245.0970 $[M + H]^+$ (calcd for 245.0972, $C_{15}H_{14}FO_2$).

1-(3-((4-Fluorobenzyl)oxy)phenyl)ethanone (2c)

Yield 87%, light yellow oil; ^{1}H NMR (500 MHz, DMSO) δ 7.59 (d, J = 7.7 Hz, 1H), 7.54 (dd, J = 7.3, 4.7 Hz, 3H), 7.47 (t, J = 7.9 Hz, 1H), 7.31 (dd, J = 8.1, 2.2 Hz, 1H), 7.25 (t, J = 8.9 Hz, 2H), 5.18 (s, 2H), 2.59 (s, 3H); ^{13}C NMR (126 MHz, DMSO) δ 198.13, 158.91, 138.82, 133.54, 133.52, 130.47, 130.40, 130.37, 121.47, 120.40, 115.83, 115.66, 114.28, 69.26, 27.28. ESI-MS m/z: 244.8 $[M + H]^+$; HRMS (ESI) m/z 245.0974 $[M + H]^+$ (calcd for 245.0972, $C_{15}H_{14}FO_2$).

1-(3-((3-Chlorobenzyl)oxy)phenyl)ethanone (2d)

Yield 81%, light yellow oil; ^{1}H NMR (500 MHz, DMSO) δ 7.59 (d, J = 7.7 Hz, 1H), 7.56 (s, 2H), 7.52–7.39 (m, 4H), 7.32 (dd, J = 8.2, 2.4 Hz, 1H), 5.22 (s, 2H), 2.59 (s, 3H); ^{13}C NMR (126 MHz, DMSO) δ 198.11, 158.78, 139.91, 138.84, 133.65, 130.86, 130.41, 128.29, 127.80, 126.65, 121.61, 120.38, 114.29, 69.04, 27.29. ESI-MS m/z: 260.9 $[M + H]^+$; HRMS (ESI) m/z 261.0678 $[M + H]^+$ (calcd for 261.0677, $C_{15}H_{14}ClO_2$).

1-(3-((4-Chlorobenzyl)oxy)phenyl)ethanone (2e)

Yield 82%, light yellow oil; ^{1}H NMR (500 MHz, DMSO) δ 7.59 (d, J = 7.7 Hz, 1H), 7.55 (d, J = 2.0 Hz, 1H), 7.54–7.43 (m, 5H), 7.30 (dd, J = 8.0, 2.2 Hz, 1H), 5.20 (s, 2H), 2.59 (s, 3H); ^{13}C NMR (126 MHz, DMSO) δ 198.11, 158.83, 138.83, 136.37, 132.98, 130.39, 129.97, 129.97, 128.95, 128.95, 121.55, 120.41, 114.28, 69.13, 27.29. ESI-MS m/z: 260.9 $[M + H]^+$; HRMS (ESI) m/z 261.0676 $[M + H]^+$ (calcd for 261.0677, $C_{15}H_{14}ClO_2$).

1-(3-((3-Bromobenzyl)oxy)phenyl)ethanone (2f)

Yield 87%, light yellow oil; ^{1}H NMR (500 MHz, DMSO) δ 7.71 (s, 1H), 7.59 (d, J = 7.7 Hz, 1H), 7.58–7.53 (m, 2H), 7.49 (dd, J = 15.9, 7.8 Hz, 2H), 7.39 (t, J = 7.8 Hz, 1H), 7.32 (dd, J = 8.1, 2.3 Hz, 1H), 5.22 (s, 2H), 2.59 (s, 3H); ^{13}C NMR (126 MHz, DMSO) δ 198.11, 158.78, 140.16, 138.84, 131.20, 131.15, 130.70, 130.42, 127.06, 122.20, 121.61, 120.38, 114.30, 68.99, 27.29. ESI-MS m/z: 306.9 $[M + H]^+$; HRMS (ESI) m/z 326.9994 $[M + Na]^+$ (calcd for 326.9991, $C_{15}H_{13}BrNaO_2$).

1-(3-((4-Bromobenzyl)oxy)phenyl)ethanone (2g)

Yield 90%, light yellow oil; ^{1}H NMR (500 MHz, DMSO) δ 7.60 (dd, J = 14.3, 8.0 Hz, 3H), 7.54 (s, 1H), 7.51–7.40 (m, 3H), 7.30 (dd, J = 8.2, 1.9 Hz, 1H), 5.19 (s, 2H), 2.59 (s, 3H); ^{13}C NMR (126 MHz, DMSO) δ 198.10, 158.81, 138.83, 136.80, 131.87, 131.87, 130.39, 130.27, 130.27, 121.56, 121.49, 120.41, 114.28, 69.16, 27.29. ESI-MS m/z: 306.9 $[M + H]^+$; HRMS (ESI) m/z 326.9990 $[M + Na]^+$ (calcd for 326.9991, $C_{15}H_{13}BrNaO_2$).

1-(3-((3-Methylbenzyl)oxy)phenyl)ethanone (2h)

Yield 92%, light yellow oil; ^{1}H NMR (500 MHz, DMSO) δ 7.58 (d, J = 7.6 Hz, 1H), 7.55 (d, J = 2.2 Hz, 1H), 7.47 (t, J = 7.9 Hz, 1H), 7.35–7.24 (m, 4H), 7.17 (d, J = 6.9 Hz, 1H), 5.15 (s, 2H), 2.59 (s, 3H), 2.34 (s, 3H); ^{13}C NMR (126 MHz, DMSO) δ 198.14, 159.06, 138.81, 138.11, 137.21, 130.35, 129.01, 128.83, 128.75, 125.28, 121.36, 120.34, 114.30, 70.02, 27.28, 21.46. ESI-MS m/z: 240.9 $[M + H]^+$; HRMS (ESI) m/z 241.1221 $[M + H]^+$ (calcd for 241.1223, $C_{16}H_{17}O_2$).

1-(3-((4-Methylbenzyl)oxy)phenyl)ethanone (2i)

Yield 88%, light yellow oil; ^{1}H NMR (500 MHz, DMSO) δ 7.57 (d, J = 7.7 Hz, 1H), 7.54 (d, J = 2.2 Hz, 1H), 7.46 (t, J = 7.9 Hz, 1H), 7.37 (d, J = 7.9 Hz, 2H), 7.32–7.26 (m, 1H), 7.22 (d, J = 7.8 Hz, 2H), 5.15 (s, 2H), 2.58 (s, 3H), 2.33 (s, 3H); ^{13}C NMR (126 MHz, DMSO) δ 198.14, 159.03, 138.79, 137.63, 134.25, 130.33, 129.48, 129.48, 128.27, 128.27, 121.33, 120.39, 114.31, 69.88, 27.28, 21.24. ESI-MS m/z: 240.9 $[M + H]^+$; HRMS (ESI) m/z 241.1222 $[M + H]^+$ (calcd for 241.12223, $C_{16}H_{17}O_2$).

1-(3-((3-Trifluoromethyl)oxy)phenyl)ethanone (2j)

Yield 83%, light yellow oil; ^{1}H NMR (500 MHz, DMSO) δ 7.87 (s, 1H), 7.81 (d, J = 7.5 Hz, 1H), 7.73 (d, J = 7.7 Hz, 1H), 7.67 (t, J = 7.7 Hz, 1H), 7.59 (dd, J = 9.4, 4.8 Hz, 2H), 7.49 (t, J = 7.9 Hz, 1H), 7.34 (dd, J = 8.1, 2.3 Hz, 1H), 5.32 (s, 2H), 2.59 (s, 3H); ^{13}C NMR (126 MHz, DMSO) δ 198.10, 158.77, 138.87, 132.14, 132.14, 130.43, 130.43, 130.07, 125.46, (q, J = 125.2 Hz), 121.67, 121.67, 120.41, 120.41, 114.29, 69.10, 27.27. ESI-MS m/z: 294.9 $[M + H]^+$; HRMS (ESI) m/z 317.0759 $[M + Na]^+$ (calcd for 317.0760, $C_{16}H_{13}F_3NaO_2$).

1-(3-((4-Trifluoromethyl)oxy)phenyl)ethanone (2k)

Yield 88%, light yellow oil; ^{1}H NMR (500 MHz, DMSO) δ 7.79 (d, J = 8.1 Hz, 2H), 7.72 (d, J = 8.1 Hz, 2H), 7.60 (d, J = 7.7 Hz, 1H), 7.57 (d, J = 1.9 Hz, 1H), 7.48 (t, J = 7.9 Hz, 1H), 7.33 (dd, J = 8.1, 2.2 Hz, 1H), 5.33 (s, 2H), 2.59 (s, 3H); ^{13}C NMR (126 MHz, DMSO) δ 198.08, 158.74, 142.21, 138.86, 130.44, 129.03, 128.78, 128.50, 128.50, 125.81 (q, J = 125.2 Hz), 123.63, 121.70, 120.39, 114.25, 69.07, 27.27. ESI-MS m/z: 294.9 $[M + H]^+$; HRMS (ESI) m/z 317.0762 $[M + Na]^+$ (calcd for 317.0760, $C_{16}H_{13}F_3NaO_2$).

1-(3-((3-Nitrobenzyl)oxy)phenyl)ethanone (2l)

Yield 93%, light yellow solid, m.p. 121–123 °C; ^{1}H NMR (500 MHz, DMSO) δ 8.36 (s, 1H), 8.23 (d, J = 8.1 Hz, 1H), 7.96 (d, J = 7.6 Hz, 1H), 7.74 (t, J = 7.9 Hz, 1H), 7.60 (dd, J = 9.4, 4.8 Hz, 2H), 7.49 (t, J = 7.9 Hz, 1H), 7.35 (dd, J = 8.1, 2.4 Hz, 1H), 5.37 (s, 2H), 2.60 (s, 3H); ^{13}C NMR (126 MHz, DMSO) δ 198.10, 158.65, 148.41, 139.73, 138.88, 134.53, 130.58, 130.48,

123.26, 122.50, 121.78, 120.43, 114.29, 68.70, 27.30. ESI-MS *m/z*: 271.9 $[M + H]^+$; HRMS (ESI) *m/z* 294.0739 $[M + Na]^+$ (calcd for 294.0737, $C_{15}H_{14}NNaO_4$).

1-(3-((4-Nitrobenzyl)oxy)phenyl)ethanone (2m)

Yield 81%, light yellow solid, m.p. 116–117 °C; ^{1}H NMR (500 MHz, DMSO) δ 8.29 (d, J = 8.6 Hz, 2H), 7.77 (d, J = 8.6 Hz, 2H), 7.61 (d, J = 7.7 Hz, 1H), 7.58 (s, 1H), 7.49 (t, J = 7.9 Hz, 1H), 7.34 (dd, J = 8.1, 2.1 Hz, 1H), 5.39 (s, 2H), 2.59 (s, 3H); ^{13}C NMR (126 MHz, DMSO) δ 198.08, 158.62, 147.59, 145.22, 138.88, 130.48, 128.75, 128.75, 124.10, 124.10, 121.82, 120.42, 114.25, 68.79, 27.29. ESI-MS *m/z*: 271.9 $[M + H]^+$; HRMS (ESI) *m/z* 294.0738 $[M + Na]^+$ (calcd for 294.0737, $C_{15}H_{14}NNaO_4$).

Abbreviations

MAO	Monoamine oxidase
FAD	Flavin adenine dinucleotide
CNS	Central nervous system
5-HT	5-Hydroxytryptamine
NE	Norepinephrine
DA	Dopamine
SI	Selectivity index
BBB	Blood–brain barrier
MTT	Methyl thiazolyl tetrazolium

Acknowledgements

The research work was financially supported by the Project of the National Natural Sciences Foundation of China (81573313).

References

1 K. Tipton, *Cell Biochem. Funct.*, 1986, **4**, 79–87.
2 A. Bach, N. C. Lan, D. L. Johnson, C. W. Abell, M. E. Bembenek, S.-W. Kwan, P. H. Seeburg and J. C. Shih, *Proc. Natl. Acad. Sci. U. S. A.*, 1988, **85**, 4934–4938.
3 J. Wouters, *Curr. Med. Chem.*, 1998, **5**, 137–162.
4 D. E. Edmondson, C. Binda, J. Wang, A. K. Upadhayay and A. Mattevi, *Biochemistry*, 2009, **48**, 4220–4230.
5 M. B. H. Youdim, D. E. Edmondson and K. F. Tipton, *Nat. Rev. Neurosci.*, 2006, **7**, 295–309.
6 M. Catto, O. Nicolotti, F. Leonetti, A. Carotti, A. D. Favia, R. Soto-Otero, E. Méndez-Álvarez and A. Carotti, *J. Med. Chem.*, 2006, **49**, 4912–4925.
7 J. Ma, M. Yoshimura, E. Yamashita, A. Nakagawa, A. Ito and T. Tsukihara, *J. Mol. Biol.*, 2004, **338**, 103–114.
8 M. C. Carreiras and J. L. Marco, *Curr. Pharm. Des.*, 2004, **10**, 3167–3175.
9 W. Weyler, Y.-P. P. Hsu and X. O. Breakafield, *Pharmacol. Ther.*, 1990, **47**, 391–417.
10 C. Binda, M. Li, F. Hubálek, N. Restelli, D. E. Edmondson and A. Mattevi, *Proc. Natl. Acad. Sci. U. S. A.*, 2003, **100**, 9750–9755.
11 C. L. De, M. Li, C. Binda, A. Lustig, D. E. Edmondson and A. Mattevi, *Proc. Natl. Acad. Sci. U. S. A.*, 2005, **102**, 12684–12689.
12 C. Binda, P. Newton-Vinson, F. Hubálek, D. E. Edmondson and A. Mattevi, *Nat. Struct. Biol.*, 2002, **9**, 22–26.
13 A. Bolasco, S. Carradori and R. Fioravanti, *Expert Opin. Ther. Pat.*, 2010, **20**, 909–939.
14 M. B. H. Youdim and Y. S. Bakhle, *Br. J. Pharmacol.*, 2006, **147**, S287–S296.
15 W. Y. Wu, J. J. Hou, H. L. Long, W. Z. Yang, J. Liang and D. A. Guo, *Zhonghua Yixue Zazhi*, 2014, **12**, 241–250.
16 M. Onofrj, L. Bonanni and A. Thomas, *Expert Opin. Invest. Drugs*, 2008, 1115–1125.
17 C. Gnerre, M. Catto, F. Leonetti, P. Weber, P. A. Carrupt, C. Altomare, A. Cosimo, C. Angelo and T. Bernard, *J. Med. Chem.*, 2000, **43**, 4747–4758.
18 V. Perez, M. Romera, J. M. Lizcano, J. L. Marco and M. Unzeta, *J. Pharm. Pharmacol.*, 2003, **55**, 713–716.
19 L. J. Legoabe, A. Petzer and J. P. Petzer, *Bioorg. Chem.*, 2012, **45**, 1–11.
20 W. Y. Wu, J. J. Hou, H. L. Long, W. Z. Yang, J. Liang and D. A. Guo, *Zhonghua Yixue Zazhi*, 2014, **12**, 241–250.
21 S. Belinda, J. B. Jacobus and J. P. Petzer, *Bioorg. Med. Chem. Lett.*, 2013, **23**, 1269–1273.
22 M. Letitia, J. P. Petzer and P. Anél, *Bioorg. Med. Chem. Lett.*, 2013, **23**, 5498–5502.
23 L. J. Legoabe, A. Petzer and J. P. Petzer, *Bioorg. Med. Chem. Lett.*, 2014, **24**, 2758–2763.
24 L. J. Legoabe, A. Petzer and J. P. Petzer, *Bioorg. Med. Chem. Lett.*, 2012, **22**, 5480–5484.
25 G. Esteban, J. Allan, A. Samadi, A. Mattevi, M. Unzeta, J. Marco-Contelles, C. Binda and R. R. Ramsay, *Biochim. Biophys. Acta*, 1844, **2014**, 1104–1110.
26 L. Novaroli, M. Reist, E. Favre, A. Carotti, M. Catto and P. A. Carrupt, *Bioorg. Med. Chem.*, 2005, **13**, 6212–6217.
27 K. F. Tipton, S. Boyce, J. O'Sullivan, G. P. Davey and J. Healy, *Curr. Med. Chem.*, 2004, **11**, 1965–1982.
28 L. J. Legoabe, A. Petzer and J. P. Petzer, *Eur. J. Med. Chem.*, 2012, **49**, 343.
29 N. T. Tzvetkov, S. Hinz, P. Küppers, M. Gastreich and C. E. Müller, *J. Med. Chem.*, 2014, **15**, 6679–6703.
30 S. Muzammil, A. Armstrong, L. Kang, A. Jakalian, P. Bonneau, V. Schmelmer, L. Amzel and E. Freire, *J. Virol.*, 2007, **81**, 5144–5154.
31 C. Binda, J. Wang, L. Pisani, C. Caccia, A. Carotti, P. Salvati, D. E. Edmondson and A. Mattevi, *J. Med. Chem.*, 2007, **50**, 5848–5852.
32 L. J. Legoabe, A. Petzer and J. P. Petzer, *Eur. J. Med. Chem.*, 2012, **49**, 343–353.
33 C. Gnerre, M. Catto, F. Leonetti, P. Weber, P. A. Carrupt, C. Altomare, A. Carotti and B. Testa, *J. Med. Chem.*, 2000, **43**, 4747–4758.
34 S. K. Roy, N. Kumari, S. Gupta, S. Pahwa, H. Nandanwar and S. M. Jachak, *Eur. J. Med. Chem.*, 2013, **66**, 499–507.
35 C. Lu, Q. Zhou, J. Yan, Z. Du, L. Huang and X. Li, *Eur. J. Med. Chem.*, 2013, **62**, 745–753.
36 E. Rudinger-Adler and J. Büchi, *Arzneim. Forsch.*, 1979, **29**, 1326–1331.

37 P. Traxler, U. Trinks, E. Buchdunger, H. Mett, T. Meyer, M. Müller, U. Regenass, J. Rösel and N. Lydon, *J. Med. Chem.*, 1995, **38**, 2441–2448.

38 W. H. Song, M. M. Liu, D. W. Zhong, Y. L. Zhu, M. Bosscher, L. Zhou, D. Y. Ye and Z. H. Yuan, *Bioorg. Med. Chem. Lett.*, 2013, **45**, 4528–4531.